JOURNAL OF MATERIALS SCIENCE 27 (1992) 5727–5734

Oxidation behaviour of the sintered Si_3N_4–Y_2O_3–Al_2O_3 system

K. KOMEYA*, Y. HARUNA, T. MEGURO
Department of Materials Chemistry, Yokohama National University, Tokiwadai, Hodogayaku, Yokohama, 240, Japan

T. KAMEDA, M. ASAYAMA
New Materials Engineering Laboratory, Toshiba Corporation, Suehirocho, Tsurumiku, Yokohama, 230, Japan

The oxidation behaviour of silicon nitride composed of Si_3N_4, Y_2O_3, Al_2O_3, AlN and TiO_2 was investigated in dry and wet air at 1100–1400 °C. The oxidation rates were confirmed to obey the parabolic law. An activation energy of 255 kJ mol^{-1} was calculated from the Arrhenius plots of the results of oxidation in an air flow. In still air the oxidation rate was larger than that in an air flow, but the oxidation rate in flowing air was not affected by the air flow rate. α-cristobalite and $Y_2O_3 \cdot 2SiO_2$ were formed in oxidized surface layers. These crystal phases increased with increasing oxidation temperature. In particular, a higher content of α-cristobalite was obtained in still air oxidation. The existence of water vapour in flowing air greatly promoted the oxidation.

1. Introduction

Silicon nitride (Si_3N_4) is an excellent material which is characterized by good thermal shock resistance and high strength. In addition, it is also an excellent oxidation-resisting material, because an SiO_2 layer forms on the surface in oxygen-containing atmospheres and this inhibits further oxidation. Therefore, the development towards practical applications as engineering ceramics have been promoted over the last 20 years.

In general, some sintering aids, such as MgO [1], Y_2O_3–Al_2O_3 [2], etc., are used to attain densification. As is well known, the additives form glassy phases by reaction with Si_3N_4 and SiO_2 existing on the surface, and liquid-phase sintering proceeds through the glassy phase. However, the existence of grain-boundary phases in silicon nitride ceramics causes a strength degradation at high temperatures and also affects the oxidation behaviour. For example, Si_3N_4 containing several per cent of Y_2O_3 and Al_2O_3, forms a grain-boundary phase consisting of the system Si–Y–Al–O–N, which is responsible for lowering the strength. To improve the high-temperature strength, the use of other additives [3] and grain-boundary crystallization methods have been investigated [4, 5].

At present, there are many kinds of commercial grade silicon nitride ceramics with different additives and compositions. This fact complicates the understanding of this material's properties. Because oxidation is affected by grain-boundary phase, as described above, the oxidation behaviour is quite complicated.

The oxidation behaviour of Si_3N_4 at high temperatures has been studied [6–12] by many researchers, but the characterization and mechanism have not been clarified. More detailed studies must be done to expand the areas of application. The effect of water vapour on oxidation is another important factor in heat engine and gas turbine applications, but few studies on this have been performed [13, 14]. This paper is concerned with the oxidation behaviour of a typically selected silicon nitride composed of Si_3N_4, Y_2O_3, Al_2O_3, AlN and TiO_2 conducted under conditions of a dry air flow with and without water vapour.

2. Experimental procedure

2.1. Specimens

Pressureless sintered Si_3N_4 containing some aids (Y_2O_3, Al_2O_3, AlN and TiO_2) was used. The characteristic properties, scanning electron micrographs and X-ray diffraction profiles of this material are listed in Table I and shown in Figs 1 and 2, respectively. As can be seen in the figures, this material is found to be composed of mainly elongated β-Si_3N_4 grains and glassy phase consisting of the system Y–Si–Al–O–N. Table I shows that the properties of the material prepared in this work are almost the same as a commercial grade material. For oxidation experiments, rectangular bars, 3 mm × 4 mm × 20 mm in size, were cut from the sintered bodies and machined using a 400

TABLE I Composition and properties of the sintered specimen

Composition	Density (g cm^{-3})	Bend strength (kg mm^{-2})		Fracture toughness, K_{1c} (MPa m$^{1/2}$)
		σ_{RT}	σ_{1200}	
Si_3N_4, Y_2O_3, Al_2O_3, AlN, TiO_2	3.22	90	45	6–7

*Concurrent with Kanagawa Academy of Science and Technology.

0022–2461

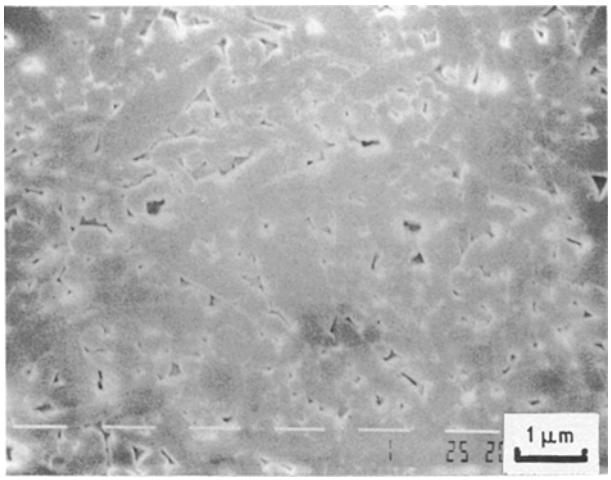

Figure 1 Micrograph of the original specimen (polished and etched).

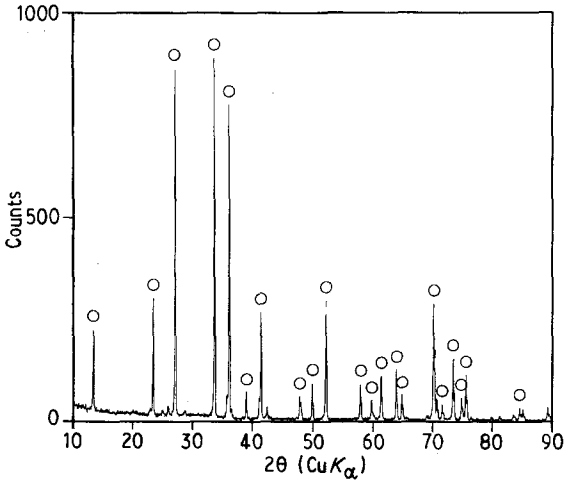

Figure 2 XRD profile of the original specimen. (○): β-Si_3N_4.

grid diamond wheel. These specimens were rinsed with acetone and ethanol before oxidation.

2.2. Oxidation

Fig. 3 shows a schematic diagram of the oxidation apparatus. The specimen on a silicon carbide plate in the centre of a high purity alumina tube was oxidized in an air flow of 0.5 l min^{-1} at 1100, 1200, 1300 and 1400 °C for 2, 6, 12, 30 and 54 h, respectively. Experiments were also performed at 1300 °C at 1.0 l min^{-1}, in still air and in wet air with 2.3, 20, 30 and 50 vol % H_2O. Dry and wet air were introduced in the direction of the arrow. Wet air bubbled through water at various temperatures was used. After oxidation, the specimen was weighed and its surface was analysed by X-ray diffraction (XRD) and electron probe microanalysis (EPMA). Surface features were also evaluated from the electron micrographs and surface roughness.

3. Results and discussion

3.1. Oxidation in dry air

Weight gain as a function of (oxidation time)$^{1/2}$, which is based on the results of tests performed under an air flow of 0.5 and 1 l min^{-1} at 1100 to 1400 °C, is shown in Fig. 4. The weight gain increases with increasing temperatures. Judging from the fact that the weight

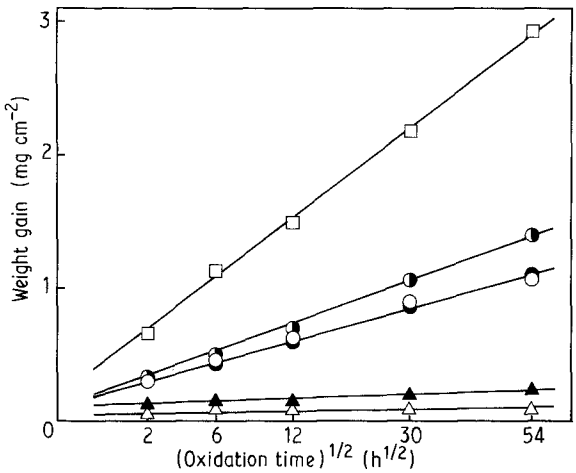

Figure 4 Palabolic plots of oxidation, in air flows of (△) 0.5 l min^{-1} at 1100 °C, (▲) 0.5 l min^{-1} at 1200 °C, (●) 0.5 l min^{-1} at 1300 °C, (○) 1 l min^{-1} at 1300 °C, (□) 0.5 l min^{-1} at 1400 °C, and (◑) in still air at 1300 °C.

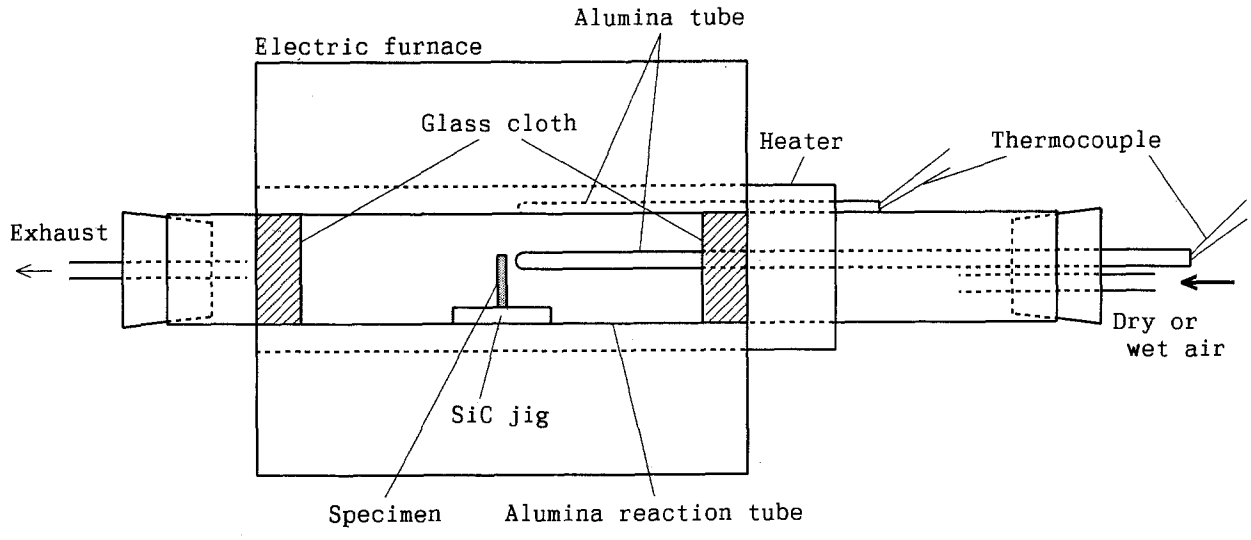

Figure 3 Schematic diagram of the oxidation apparatus.

TABLE II Comparison of activation energies

System	Temperature range (°C)	Activation energy ($kJ\,mol^{-1}$)	Reference
Pressureless sintering Si_3N_4 in air flow	1100–1400	255	Present work
Hot-pressed Si_3N_4 in O_2	1000–1400	375	[7]
Hot-pressed Si_3N_4 in 16 kPa dry air	1248–1458	440	[8]
Hot-pressed Si_3N_4 in flowing dry air	1100–1400	385	[12]
Sintered Si_3N_4 in wet nitrogen atmosphere at 20 kPa	1200–1300	800	[14]
Hot-pressed Si_3N_4 in 150 torr dry O_2	1300–1450	293	[15]
Hot-pressed Si_3N_4 in wet air	1200–1400	488 ± 30	[16]
Powder Si_3N_4 in O_2	1065–1340	256	[17]
Powder Si_3N_4 in air	1065–1340	285	[17]
Powder Si_3N_4 in O_2 or air	1100–1300	147	[18]

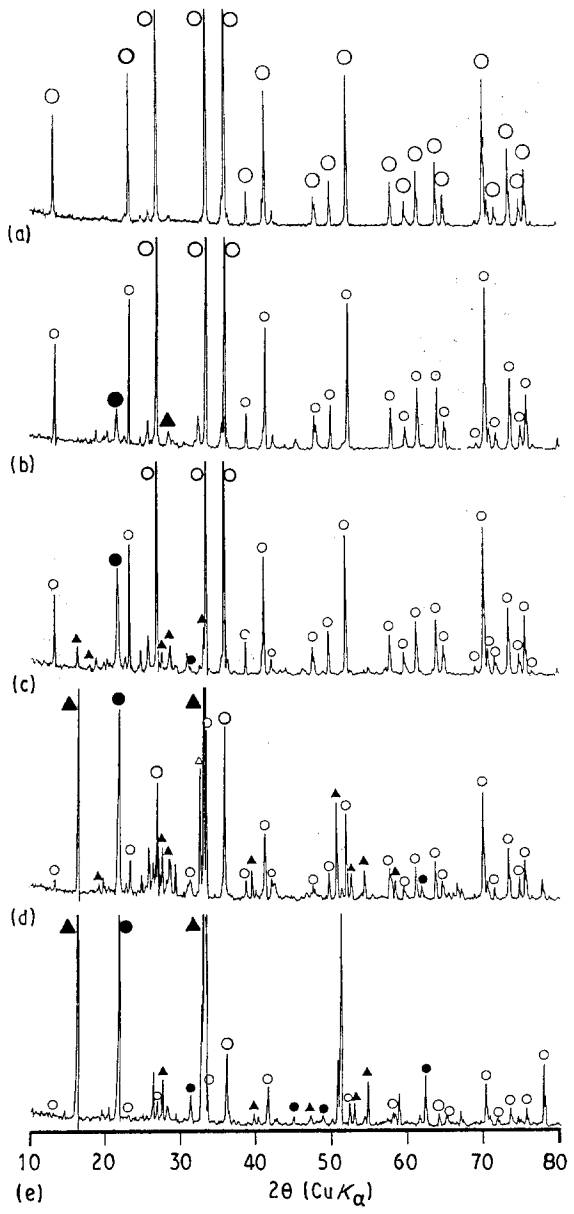

Figure 5 XRD profiles (a) before and (b–e) after oxidation for 54 h in an air flow of $0.5\,l\,min^{-1}$. (a) Before oxidation, (b) 1100 °C, (c) 1200 °C, (d) 1300 °C, (e) 1400 °C. (○) β-Si_3N_4, (▲) $Y_2O_3 \cdot 2SiO_2$, (●) α-cristobalite.

gain rapidly increases over 1300 °C, it is considered that the oxidation resistance decreases in that temperature range. No effect of flow rate on oxidation was found, but in still air the oxidation rate was larger than that in flowing air. This difference is thought to be based on the formation of an oxidation protective layer. Probably, the more protective layer seems to be formed in dry air-flow oxidation, compared with in still air.

From the good linearity of the plots in Fig. 4, except in the early stage, the oxidation is seen to obey the parabolic law, indicating that the diffusion is the rate-determining step. An activation energy of $255\,kJ\,mol^{-1}$ was calculated from the Arrhenius plots of linear slopes in Fig. 4. In order to compare this value with that reported by other researchers [7, 8, 12, 14–18], activation energies for sintered or powdered specimens are listed in Table II. The value obtained in this work is relatively low. The effect of TiO_2 addition may be involved, but the details are obscure.

XRD profiles of the specimen surfaces before and after oxidation are shown in Fig. 5. It is seen that the

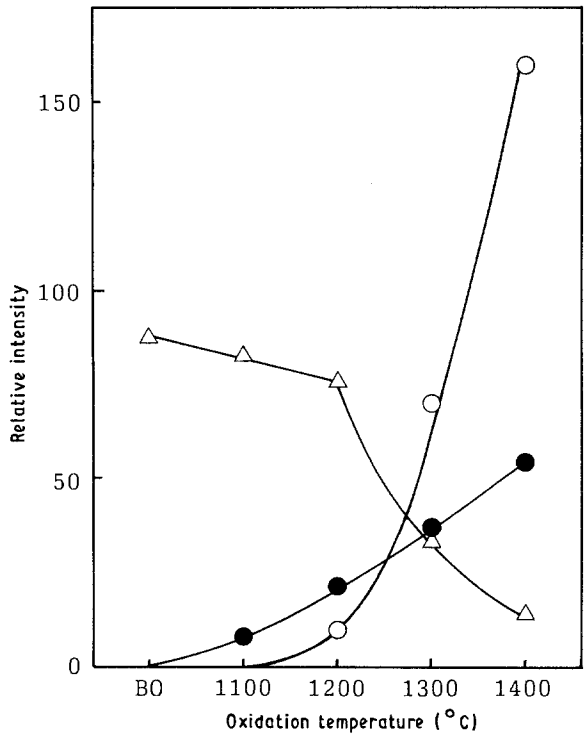

Figure 6 Phase changes during oxidation at various temperatures for 54 h in an air flow of $0.5\,l\,min^{-1}$. (△) β-Si_3N_4, (○) $Y_2O_3 \cdot 2SiO_2$, (●) α-cristobalite. BO, before oxidation.

crystal phases present depend on the oxidation temperatures. Fig. 6 represents the relative intensities of β-Si_3N_4, α-cristobalite and $Y_2O_3 \cdot 2SiO_2(Y_2S)$ [1] which are calculated from the profiles of Fig. 5. The amounts of α-cristobalite and Y_2S formed increase with increasing temperature, which is especially remarkable over 1300 °C. A tendency to produce more Y_2S than α-cristobalite at high temperatures is observed. In experiments at 1300 °C, almost no effect of flow rate on the content of each phase was found.

Fig. 7 demonstrates the relation between reaction temperatures and surface roughness after oxidation. The maximum value of surface roughness, R_{max}, measured by the contact profile method, was plotted in the figure. R_{max} is helpful in confirming the extent of oxidation: it becomes higher with increasing temperature, indicating that devitrification of silicate glass proceeds in the early stage. In the case of still-air oxidation, R_{max} was larger than that in a dry air flow.

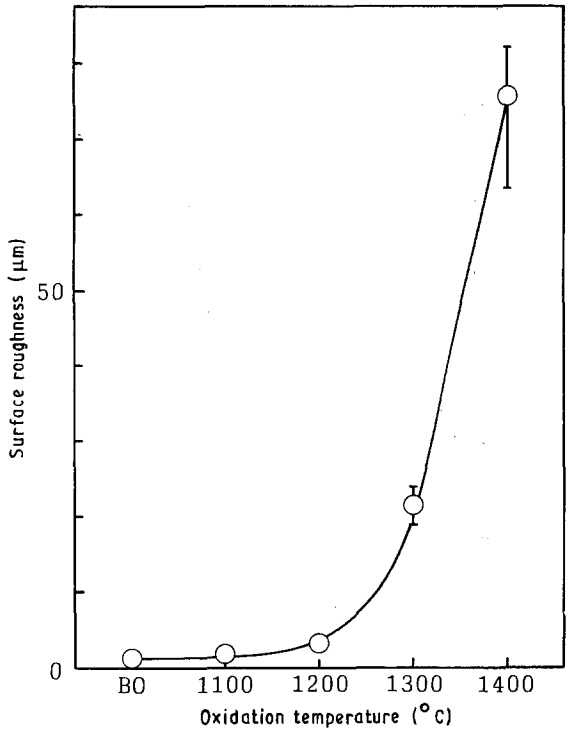

Figure 7 Relationship between surface roughness and temperature of oxidation in an air flow of 0.5 l min^{-1} for 54 h. BO, before oxidation.

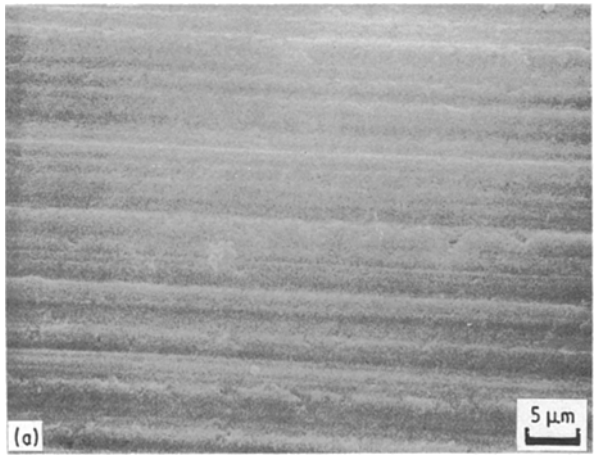

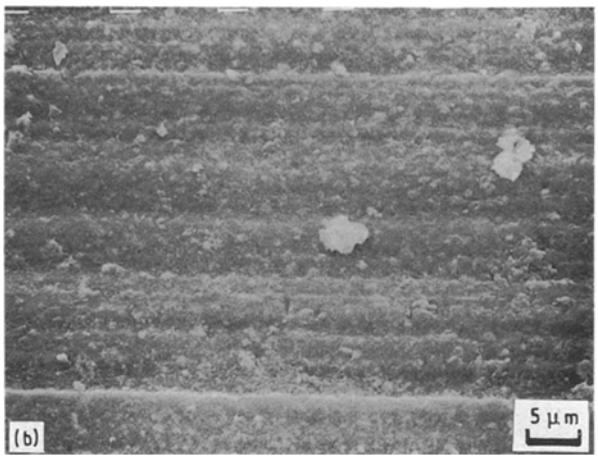

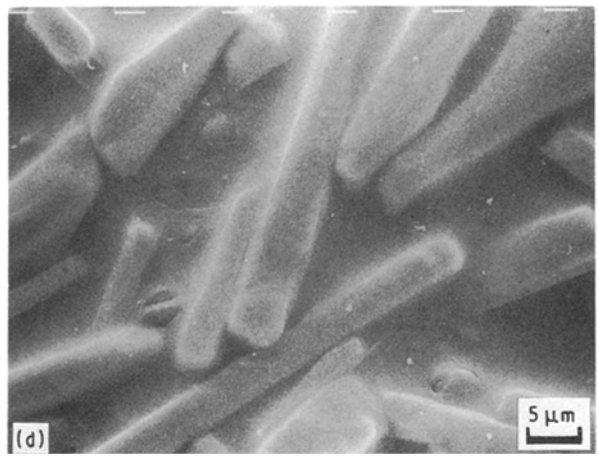

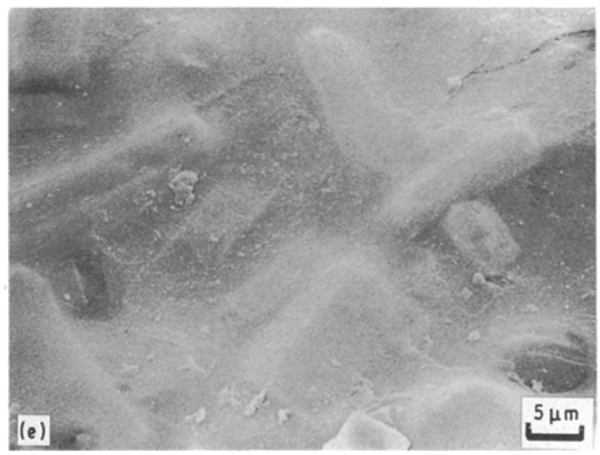

Figure 8 Micrographs of oxidized specimens in an air flow of 0.5 l min^{-1} for 54 h (a) Original specimen, (b) 1100 °C, (c) 1200 °C, (d) 1300 °C, (e) 1400 °C.

No effect of flow rate on R_{max} was observed, which agrees with the results of Fig. 5.

Fig. 8 shows scanning electron micrographs of the specimens before and after oxidation. The surface of the specimen oxidized at 1100 °C is almost the same as the original, remaining the machining flaws. Above 1200 °C oxidation, glass-like smooth and flat surfaces, including some crystals, are observed. Plate-like crystals, considered to be Y_2S [19], are clearly observed in specimens of 1300 °C oxidation. The development of crystals is also recognized at 1400 °C.

Fig. 9 shows X-ray images of the cross-section of the specimens oxidized in an air flow of 0.5 l min^{-1} at 1300 °C for 54 h. Elemental titanium and aluminium are concentrated in the oxidized layer. It can be speculated [20] that because a concentration gradient of elements between the oxidized surface and the grain-boundary phase acts as a driving force, yttrium and aluminium move to the surface through the grain-boundary phase, and consequently a compound of Y_2S was formed. Despite high aluminium concentration in the surface, no aluminium compound was

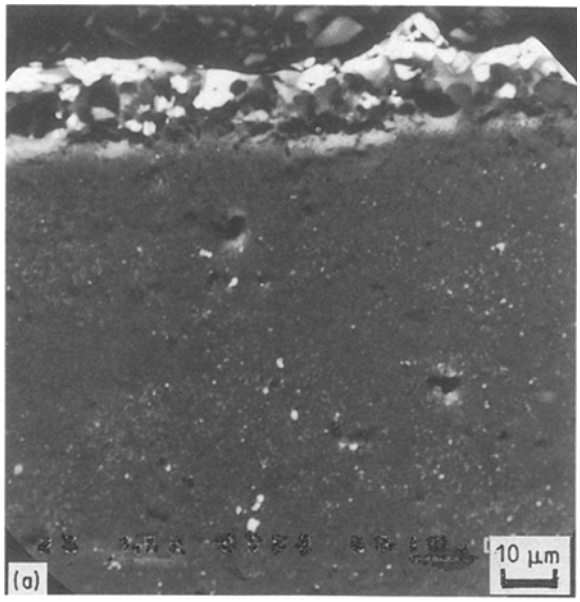

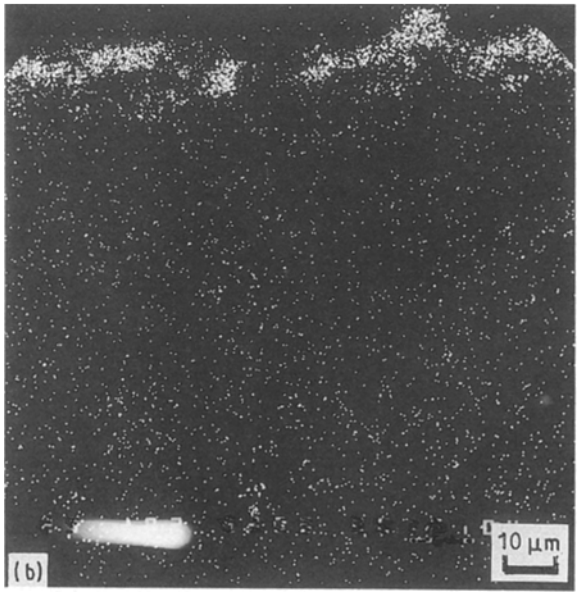

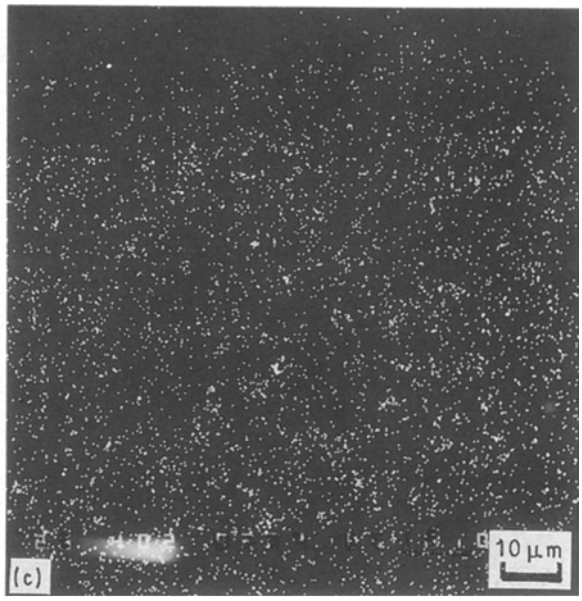

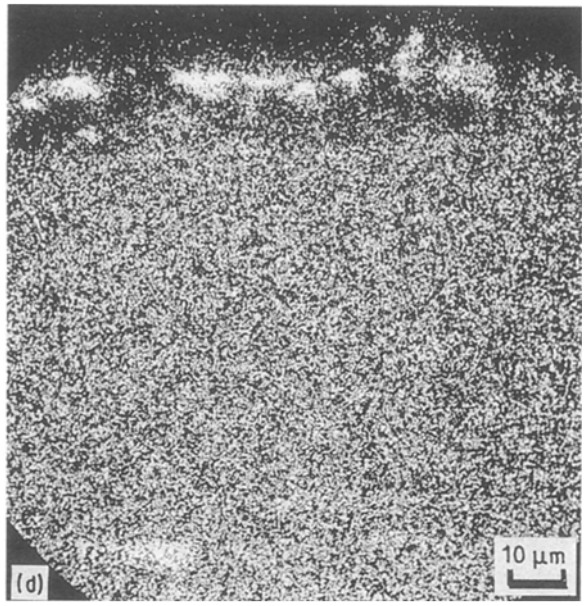

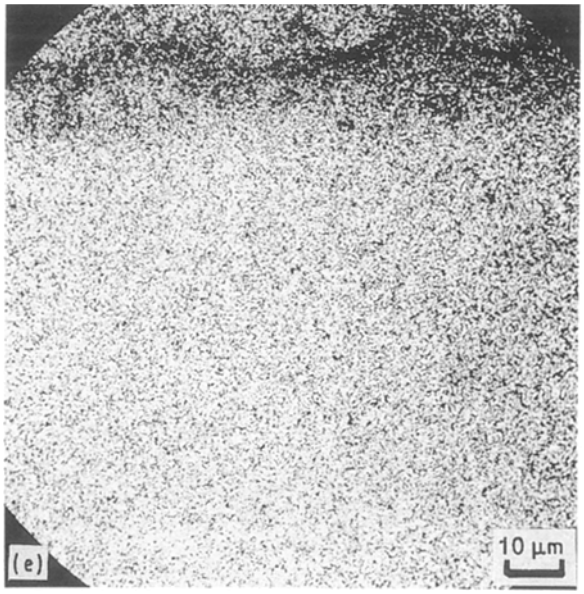

Figure 9 EPMA photographs of specimens oxidized at 1300 °C in an air flow of 0.5 l min^{-1} for 54 h. (a) Composition image, (b) X-ray image of yttrium, (c) X-ray image of titanium, (d) X-ray image of aluminium, (e) X-ray image of silicon.

detected by XRD. Therefore it is considered that aluminium exits in the glassy phase. The concentration of silicon near the surface is relatively low compared with the internal distribution, because silicon should be diluted within the oxidation layer.

3.2. Oxidation in wet air

The oxidation dependence of the weight gain of the specimens oxidized in dry and wet air flows at 1300 °C is shown in Fig. 10. The figure illustrates that weight gain in a wet air flow is larger than that in a dry air flow, and that the weight gain increases with increasing H_2O concentration. The mechanism of oxidation in wet air is not clear, but the results in Fig. 10 suggest that water vapour significantly participates in the oxidation.

Fig. 11 shows the relative intensities obtained from XRD profiles of β-Si_3N_4, α-cristobalite and Y_2S in the oxidized layer. The essential difference between the crystal phases oxidized in dry and wet air flows is in the quantity of α-cristobalite and Y_2S crystals. A moist atmosphere results in a decrease of Y_2S and a simultaneous increase of α-cristobalite and with increasing H_2O concentration the amount of α-cristobalite increases and that of Y_2S slightly decreases. It can be assumed that water vapour acts as a catalyst and promotes devitrification of silicate glass.

As shown in Fig. 12, R_{max} of the specimens oxidized in a wet air flow. Moreover, there was a tendency for the crystals to grow larger in R_{max} with increasing H_2O concentration, which corresponds to the XRD results.

Fig. 13 shows scanning electron micrographs of the oxidized surfaces in wet air. From these results, in the case of wet-air oxidation, irregular crystal shapes (arrowed in Fig. 13b) are observed, which can be compared with the plate-like crystal features in dry-air oxidation (Fig. 13a). This indicates that the Y_2S crystal shapes are strongly affected by the presence of water vapour during oxidation.

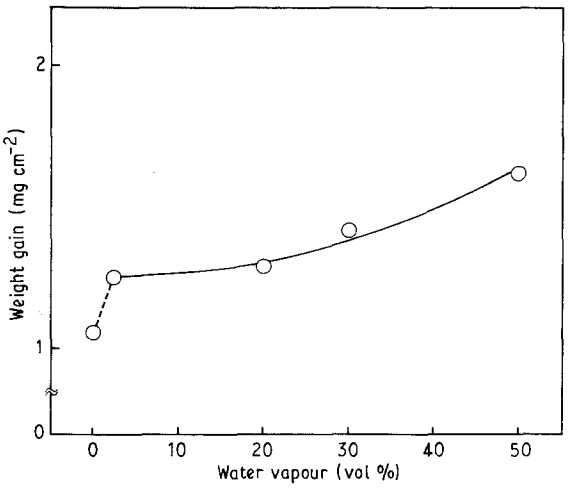

Figure 10 Weight gain after 54 h oxidation at 1300 °C in an air flow (0.5 l min^{-1}) containing water vapour.

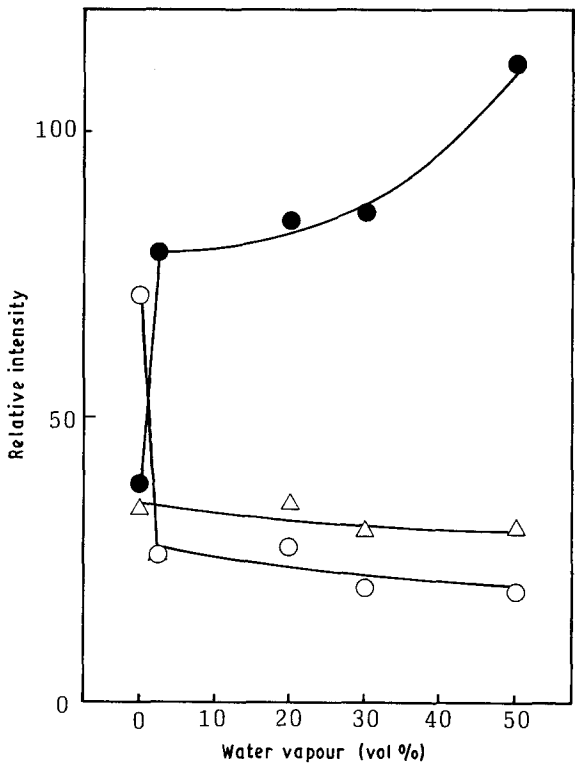

Figure 11 Phase changes during 54 h oxidation at 1300 °C in an air flow (0.5 l min^{-1}) containing water vapour. (△) β-Si_3N_4, (○) $Y_2O_3 \cdot 2SiO_2$, (●) α-cristobalite.

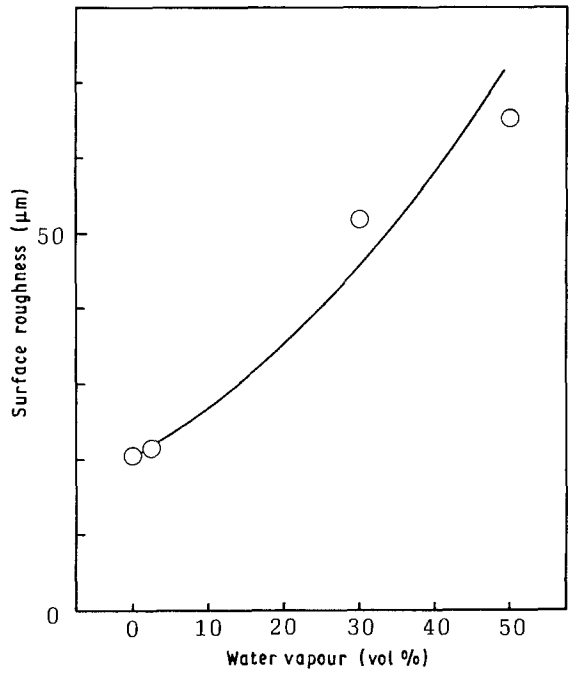

Figure 12 Surface roughness after 54 h oxidation at 1300 °C in an air flow (0.5 l min^{-1}) containing water vapour.

4. Conclusions

The oxidation behaviour of typically selected sintered silicon nitride composed of Si_3N_4, Y_2O_3, Al_2O_3 and TiO_2 was investigated in dry and wet air at 1000–1400 °C. The following conclusions were drawn.

1. Oxidation rates were confirmed to obey the parabolic law, accompanied by the migration of Y–Al–Ti–O–N grain-boundary phase to the surface.

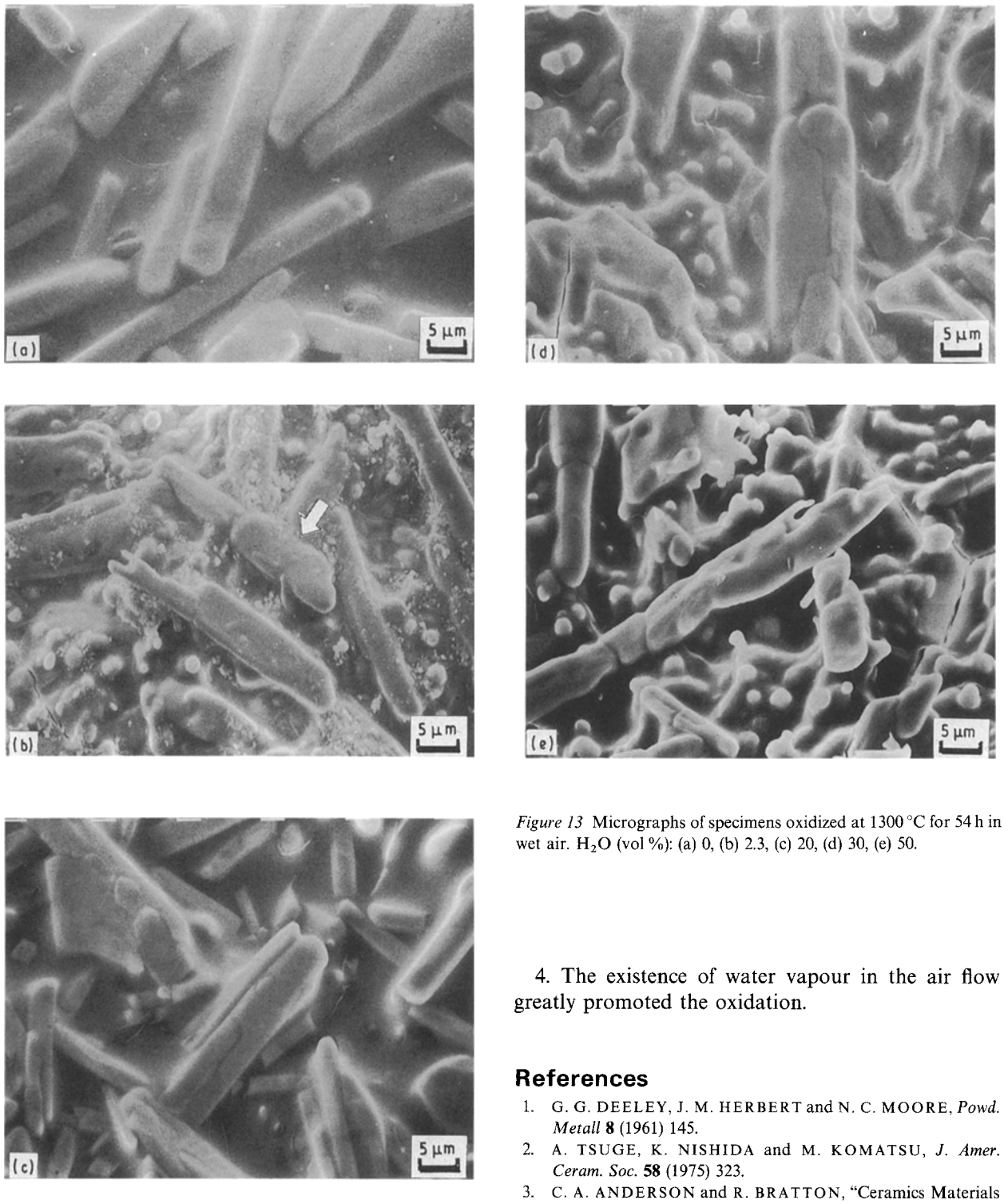

Figure 13 Micrographs of specimens oxidized at 1300 °C for 54 h in wet air. H_2O (vol %): (a) 0, (b) 2.3, (c) 20, (d) 30, (e) 50.

However, the role of the titanium contained in this material has not been clarified. An activation energy of 255 kJ mol^{-1} was calculated from the Arrhenius plots of oxidation rates in an air flow.

2. The oxidation rate in still air was larger than that in an air flow because a good protective oxidized layer is difficult to form. However, the oxidation rate in flowing air was not affected by the flow rate.

3. α-cristobalite and $Y_2O_3 \cdot 2SiO_2$ were formed in the oxidized surface layers. These crystal phases increased with increasing temperature, and a higher content of α-cristobalite was obtained in still air oxidation.

4. The existence of water vapour in the air flow greatly promoted the oxidation.

References

1. G. G. DEELEY, J. M. HERBERT and N. C. MOORE, *Powd. Metall* **8** (1961) 145.
2. A. TSUGE, K. NISHIDA and M. KOMATSU, *J. Amer. Ceram. Soc.* **58** (1975) 323.
3. C. A. ANDERSON and R. BRATTON, "Ceramics Materials for High Temperature Turbines", Final Technical Report, US Energy Research and Development Adm. Contract EY-76-C-05-5210, August 1977.
4. A. TSUGE and K. NISHIDA, *Amer. Ceram. Soc. Bull.* **57** (1978) 424.
5. K. KOMEYA, M. KOMATSU, T. KAMEDA, Y. GOTO and A. TSUGE, *J. Mater. Sci.* **26** (1991) 5513.
6. F. F. LANGE, S. C. SINGHAL and C. KUZNICKI, *J. Amer. Ceram. Soc.* **60** (1975) 249.
7. S. C. SINGHAL, *J. Mater. Sci.* **11** (1976) 500.
8. D. CUBICCIOTI and K. H. LAU, *J. Amer. Ceram. Soc.* **61** (1978) 512.
9. C. L. QUACKENBUSH and J. T. SMITH, *Amer. Ceram. Soc. Bull.* **59** (1980) 533.
10. Y. HASEGAWA, H. TANAKA, M. TSUTSUMI and H. SUZUKI, *Yogyo-Kyokai-Shi* **88** (1980) 292.
11. Y. HASEGAWA, T. YAMANE, K. HIROTA, M. TSUTSUMI and H. SUZUKI, *ibid.* **89** (1981) 46.
12. G. N. BABINI, A. BELLOSI and P. VINCENZINI, *J. Amer. Ceram. Soc.* **64** (1981) 578.

13. M. MAEDA, K. NAKAMURA and T. OHKUBO, *J. Mater. Sci. Lett.* **24** (1989) 2120.
14. T. SATO, K. HARYU, T. ENDO and M. SHIMADA, *J. Mater. Sci.* **22** (1987) 2635.
15. W. C. TRIPP and H. C. GRAHAM, *J. Amer. Ceram. Soc.* **59** (1976) 399.
16. S. C. SINGHAL, *ibid.* **59** (1976) 81.
17. R. M. HORTON, *ibid.* **52** (1969) 121.
18. P. GOURSAT, P. LORTHOLARY, D. TETARD and M. BILLY, in "Proceedings of the 7th International Symposium on Reactivity of Solids", Bristol (1972) p. 315.
19. G. N. BABINI, A. BELLOSI and P. VINCENZINI, *J. Mater. Sci.* **19** (1984) 3487.
20. Y. HASEGAWA and K. HIROTA, *Ceramics* **18** (1983) 580.

Received 26 June 1991
and accepted 7 February 1992